Supplementary Figure 1

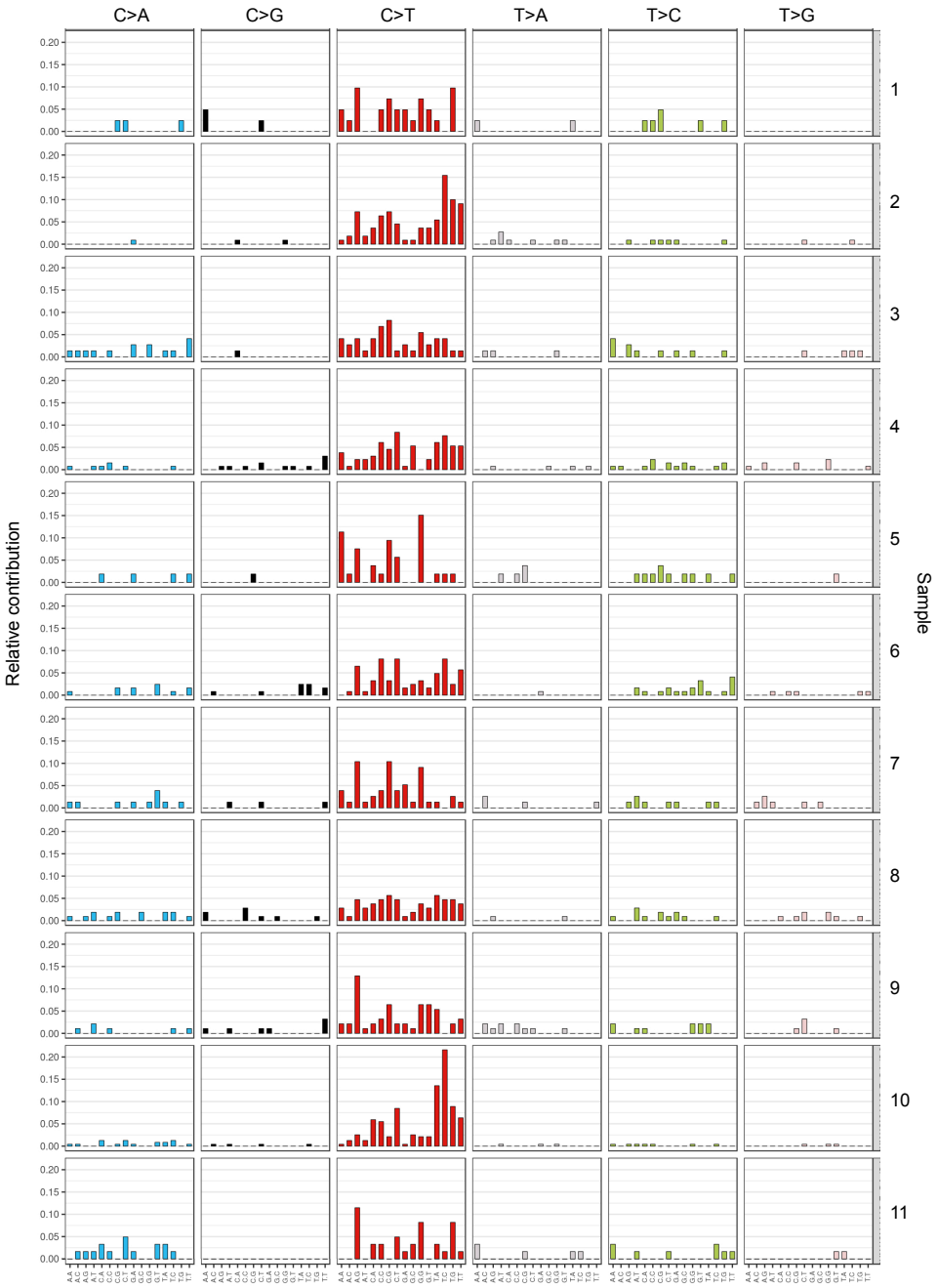

Supplementary Figure 1. Global mutational patterns in BPDCN.

Somatic DNA mutations in 11 BPDCN whole exomes compared to matching germline are shown as patients by row and base change in columns plotted as relative contribution to the total number of base changes. Mutations are grouped by the specific base change on either strand (C>A, C>G, C>T, T>A, T>C, or T>G) and each individual bar plot represents the bases flanking the mutated base. Signatures of UV-induced mutational processes are characterized by a preponderance of C>T substitutions at dipyrimidine sites, such as CC>TT.

Supplementary Figure 2

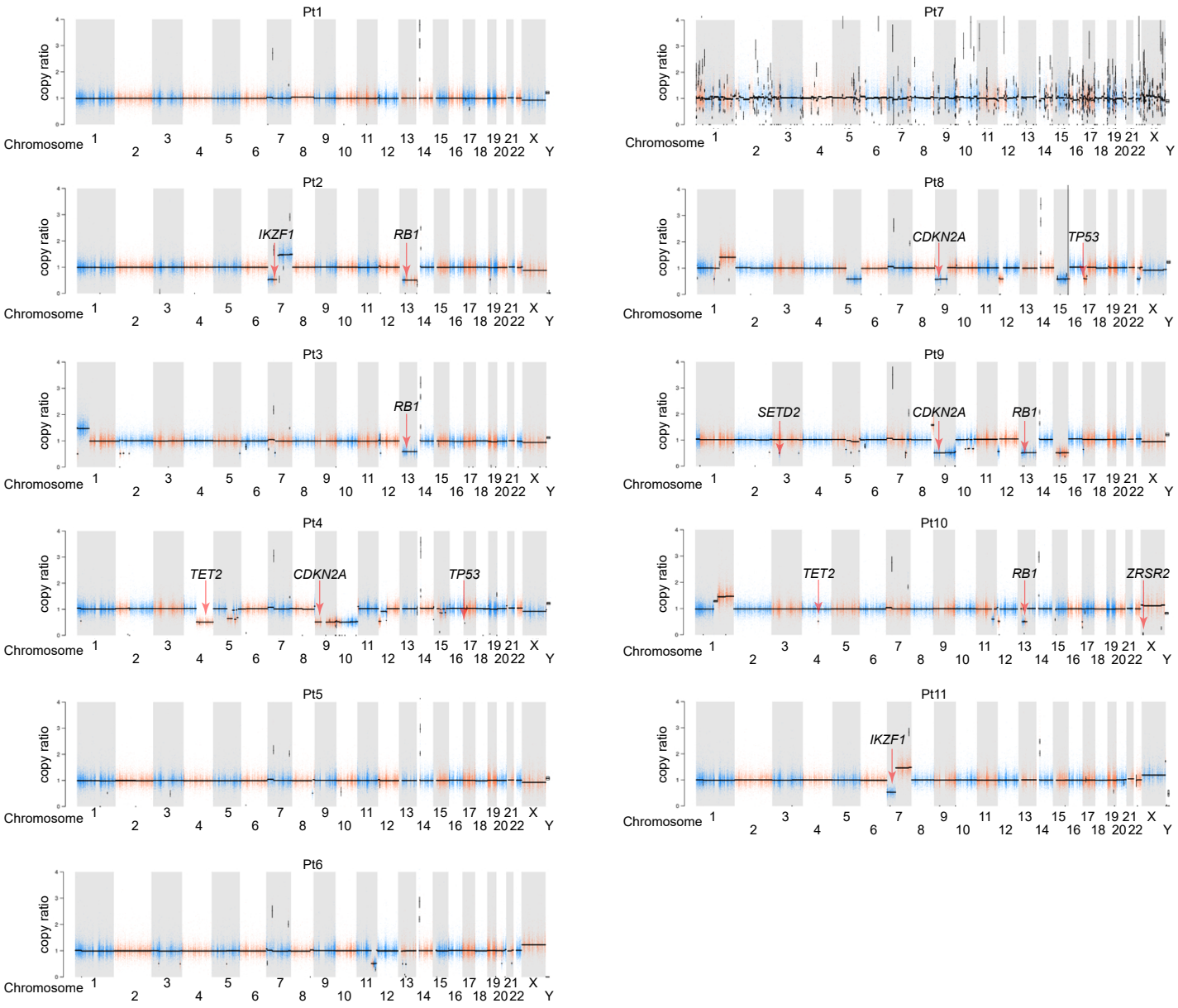

Supplementary Figure 2. Somatic alterations in DNA copy number from isolated BPDCN cells.

DNA copy ratio of tumor to normal calculated from whole exome sequencing is plotted for 11 BPDCN tumor/normal pairs by chromosome, where a copy ratio of 1 means no difference between tumor and normal, <1 is copy loss and >1 is copy gain. Chromosome positions of genes of interest are indicated.

Supplementary Figure 3

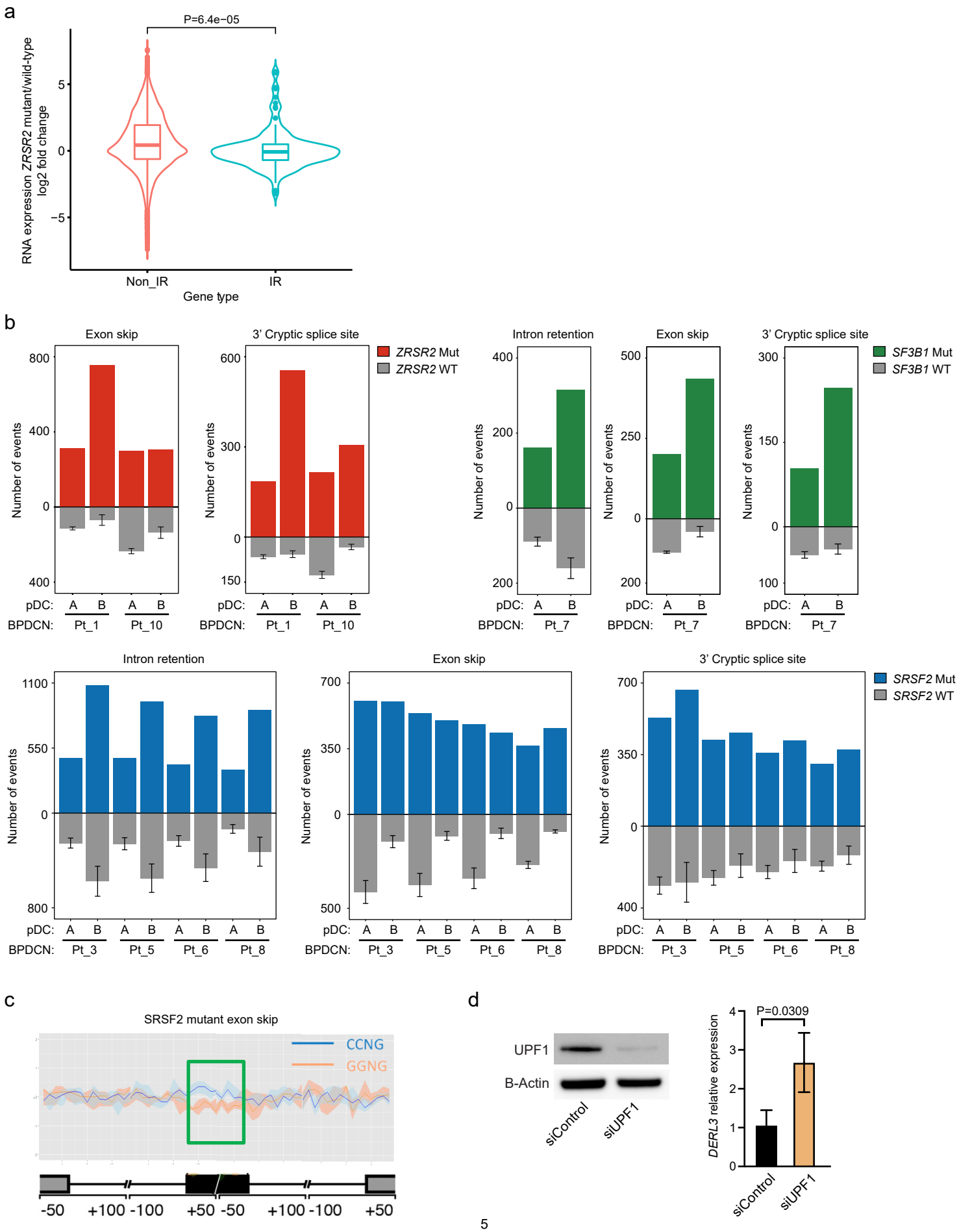

Supplementary Figure 3. Aberrant RNA splicing and gene expression in BPDCN. **a**. Log2 fold change of gene expression on a gene-by-gene basis in BPDCNs with *ZRSR2* mutations (n=2) compared to no splicing factor mutation (n=4) among genes showing aberrant intron retention (IR) versus those without (Non_IR). Groups compared by t test; box represents 25-75%ile; horizontal line in box represents the median. **b.** Mis-splicing events in the indicated BPDCN samples compared to normal donor pDCs are shown, categorized as intron retention, exon skipping, or cryptic 3' splice site events. BPDCNs with *ZRSR2* mutation (n=2), BPDCN with an *SF3B1* mutation, BPDCNs with *SRSF2* mutation (n=4), and BPDCN patients without any known splicing mutation (n=4) are shown, using $P \leq 0.05$ in the respective splicing factor mutant cases compared to normal pDCs (two independent samples, A and B) to define events. **c.** Meta-gene tracing for an *SRSF2* mutated BPDCN showing the canonical exon inclusion/exclusion pattern averaged across the genome for an exon containing a CCNG (inclusion favored) or GGNG (exclusion favored) SRSF2 RNA recognition motif (RRM), similar to that previously defined for *SRSF2* mutations in MDS. **d**. (Left) Western blot for UPF1 and beta-actin and (Right) quantitative RT-PCR for *DERL3* relative to *GAPDH* in ZRSR2 deficient CAL1 cells transfected with control siRNAs or siRNAs targeting *UPF1*, n=3 technical replicates compared by t test.

Supplementary Figure 4

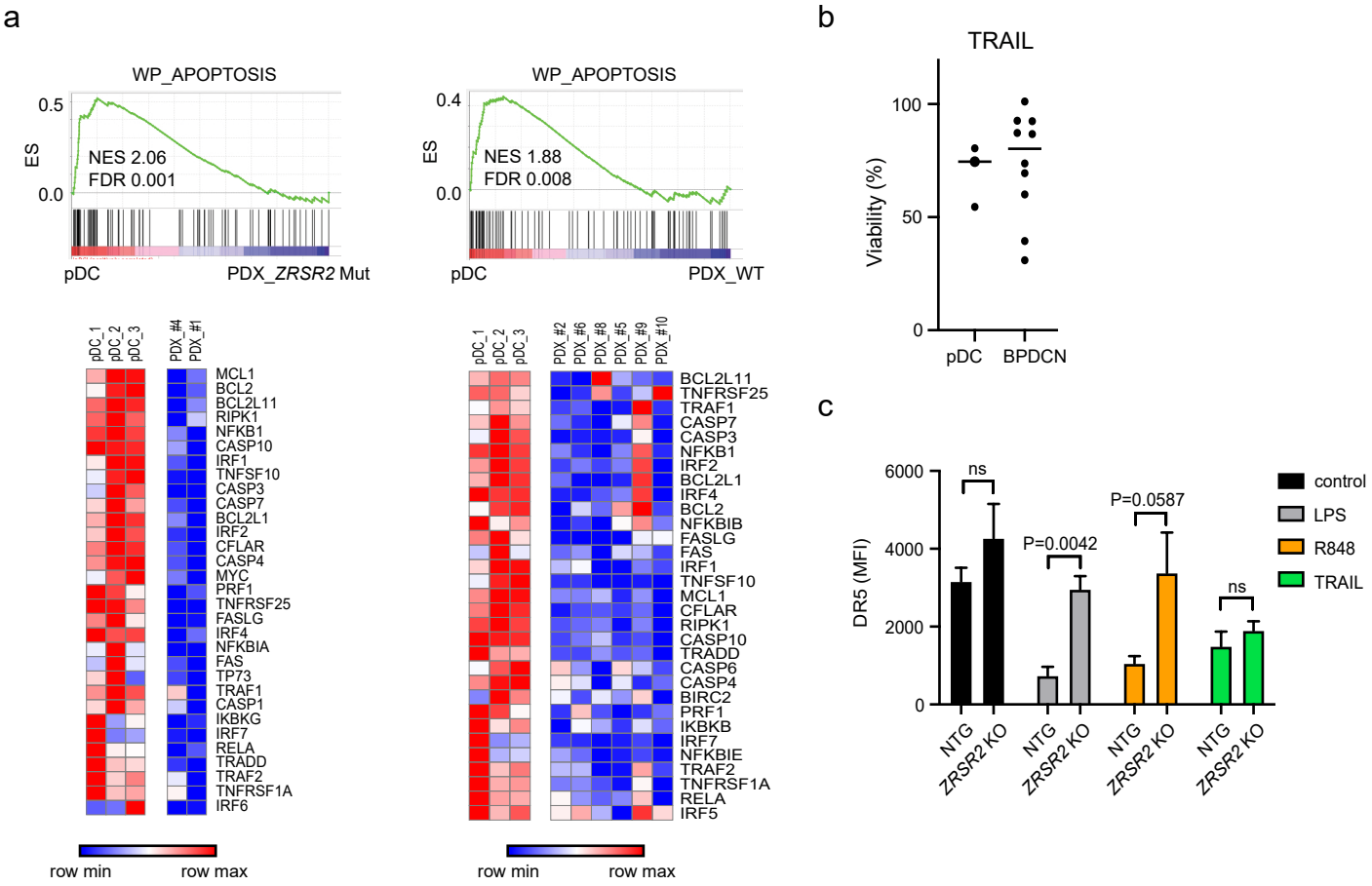

Supplementary Figure 4. Apoptosis signatures, viability, and features of TLR agonist or TRAIL treated BPDCNs, pDCs, and engineered *ZRSR2* KO cells.

a. GSEA for apoptosis signatures in pDCs (n=3) compared to BPDCN PDXs with *ZRSR2* mutation (Mut, n=2) or that lack a known splicing factor mutation (WT, n=6), each after treatment with R848. ES, enrichment score; NES, normalized enrichment score; FDR, false discovery rate. Heatmaps of the leading edge plotted as low (blue) to high (red) relative expression. **b.** Cell viability 24 hours after TRAIL treatment of pDCs or BPDCN PDXs relative to vehicle. Each dot represents an independent culture of normal donor pDCs or BPDCN cells. **c**. DR5 (TRAIL receptor) expression on the surface of control (NTG) or *ZRSR2* KO CAL1 cells after treatment with the indicated treatments: LPS, R848, or TRAIL.

Supplementary Figure 5

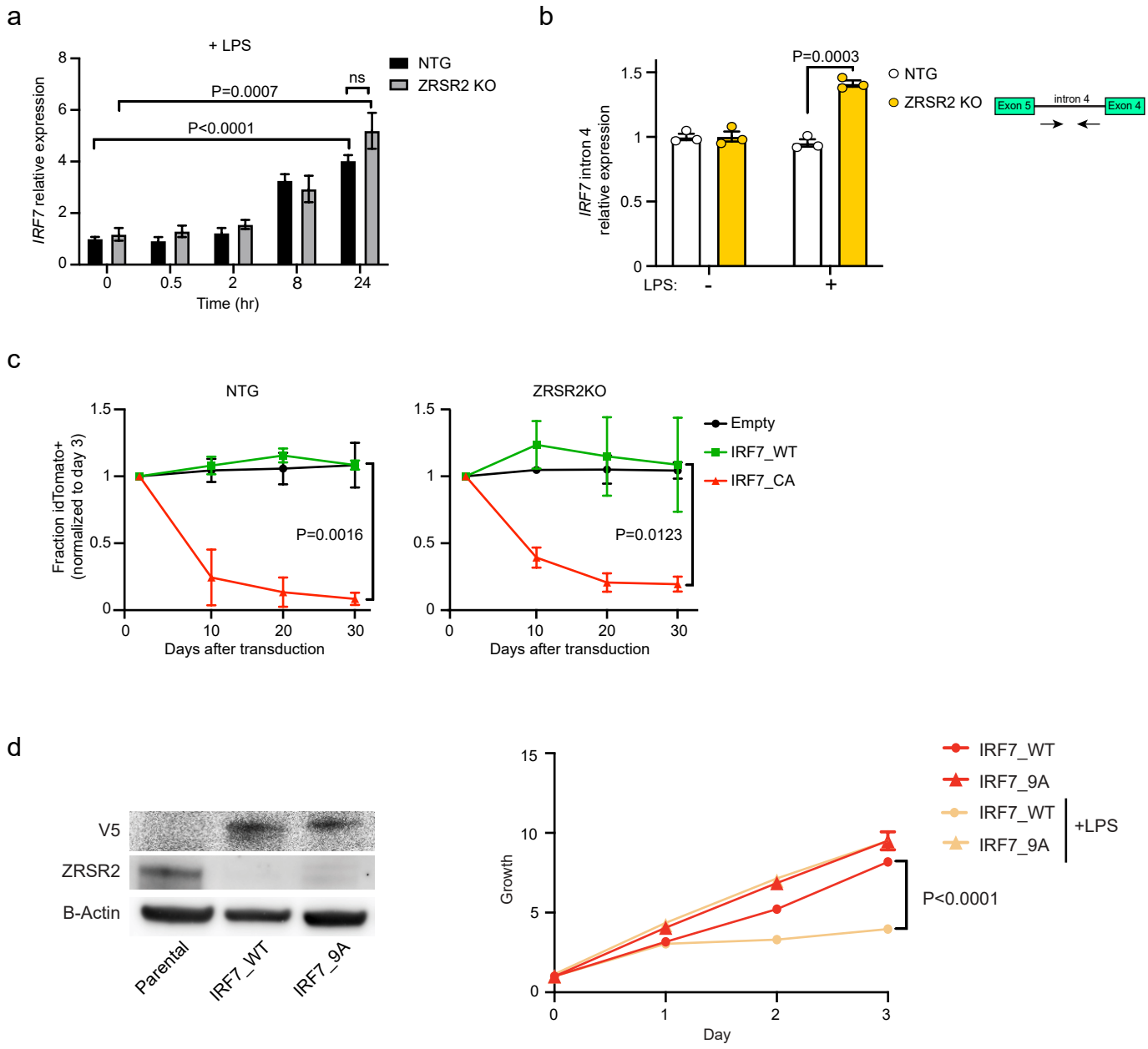

Supplementary Figure 5. Spliced active IRF7 is important for the growth disadvantage after TLR stimulation in BPDCN cells.

a. Induction of *IRF7* RNA relative to *GAPDH* in both control and *ZRSR2* knockout CAL1 cells is shown at the indicated times after stimulation with LPS. Each group represents biological triplicates compared by t test. **b**. Quantitative RT-PCR for *IRF7* intron 4 relative to *IRF7* spliced exon expression in control or *ZRSR2* knockout (KO) CAL1 cells with or without LPS treatment. **c.** idTomato positive cells relative to day 3 after transduction with empty vector, wild-type IRF7 (IRF7_WT), or constitutively active IRF7 (IRF7_CA) in CAL1 cells with control sgRNA or knockout of *ZRSR2*. Each group represents biological triplicates with IRF_WT and IRF_CA compared by t test. **d.** (Left) Western blot for V5, ZRSR2, and beta-actin in parental CAL1 cells or in CAL1 cells with a knock-in of a V5-tagged intronless IRF7 wild-type (WT) or inactive (9A) cDNA into the endogenous *IRF7* locus in *ZRSR2* knockout cells. (Right) Relative growth of knock-in IRF7_WT or IRF7_9A in *ZRSR2* KO CAL1 cells, with or without LPS treatment. Day 3 biological triplicates compared by t test.

Supplementary Figure 6

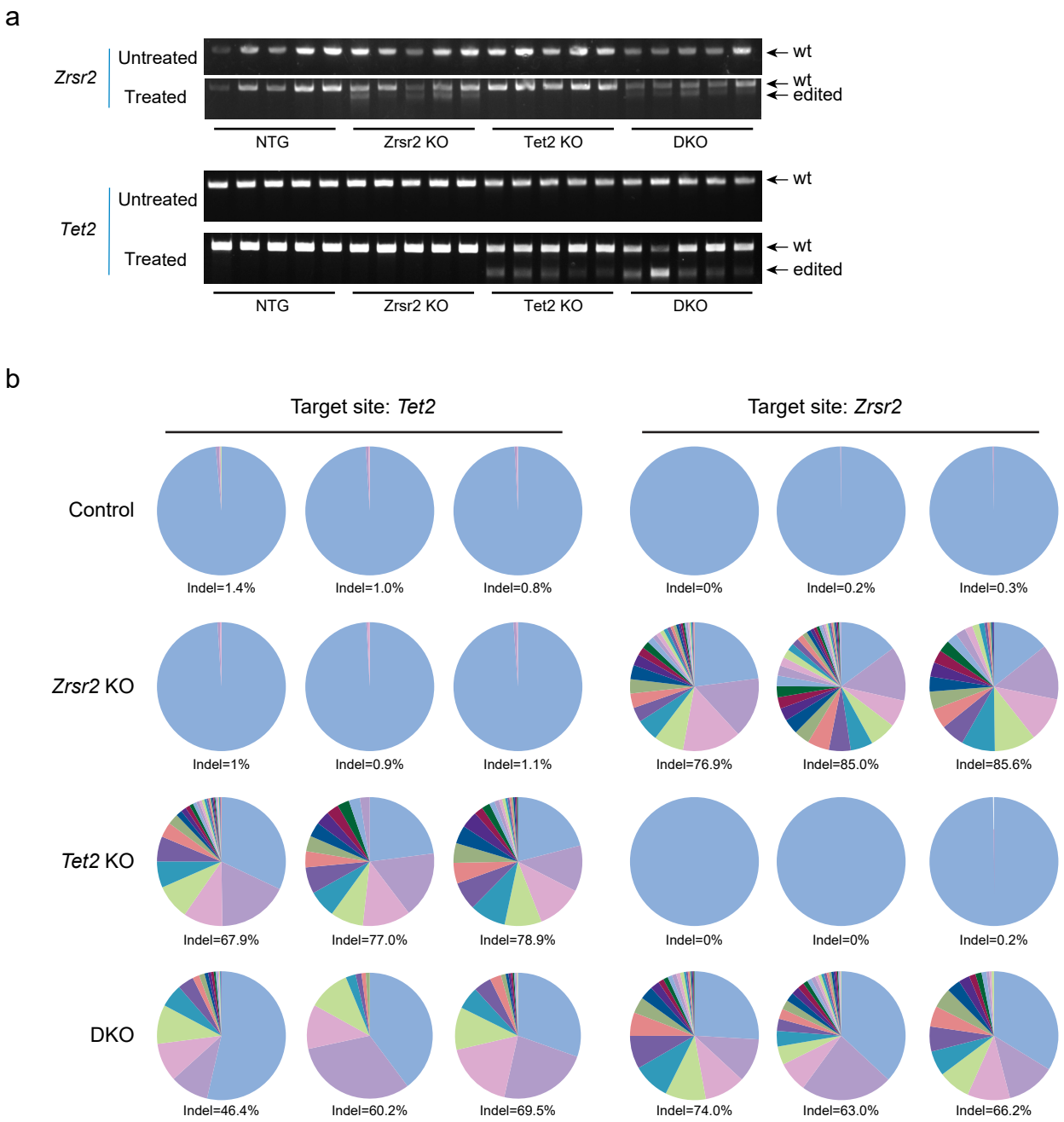

Supplementary Figure 6. Qualitative and quantitative assessments of CRISPR/Cas9 allelic disruption at the *Zrsr2* and *Tet2* loci in mouse bone marrow.

a. T7 endonuclease assay on bone marrow lineage negative, c-kit+ HSPCs from transplant recipients to detect indel mutations after CRISPR/Cas9 editing. Amplified sgRNA target sites in *Zrsr2* or *Tet2* from cells harvested from the indicated groups (n=5 independent animals/genotype) are indicated. “Untreated” and “Treated” refer to whether the PCR products were incubated with T7 endonuclease. **b**. Next-generation sequencing quantitation of indels (insertion-deletion) events at the *Tet2* or *Zrsr2* sgRNA cut sites in bone marrow cells from 3 independent animals that received bone marrow transplants with sgRNAs of the indicated genotypes. Each slice in the pie chart represents the relative representation of a distinct indel event based on DNA sequencing relative to all sequences at the site. Indel percentage indicates the percent of mutant sequences relative to the total number of sequences at the sgRNA cut site.

Supplementary Figure 7

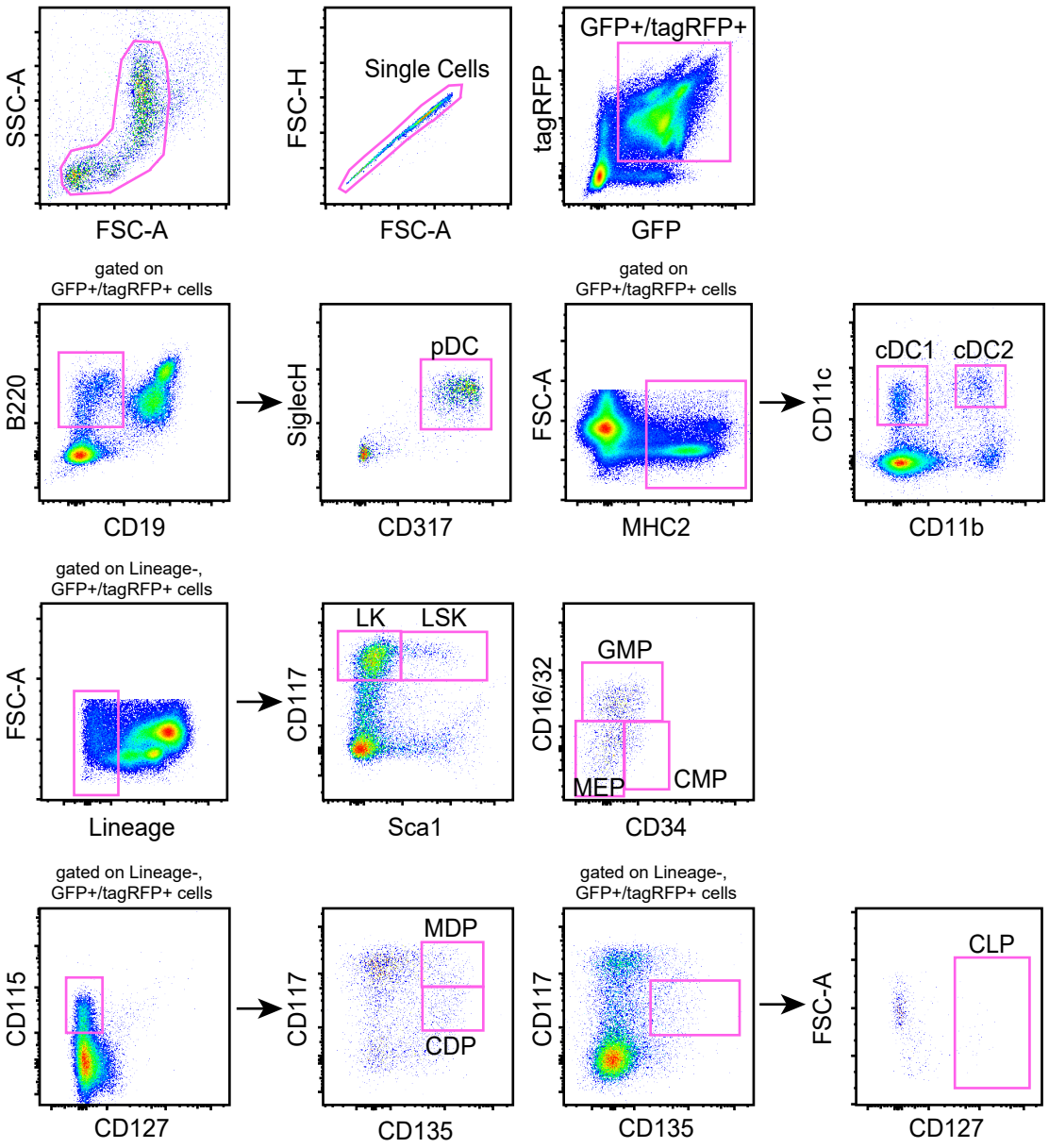

Supplementary Figure 7. Gating strategy for bone marrow HSPC and DC subpopulations. Representative flow cytometry plots are shown for mouse bone marrow to define the gating strategy used to quantify hematopoietic stem and progenitor cells (HSPCs) and mature hematopoietic cells, including cDCs and pDCs.

Supplementary Figure 8

a

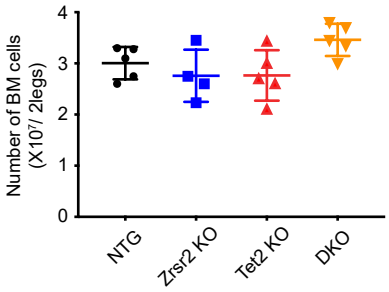

b

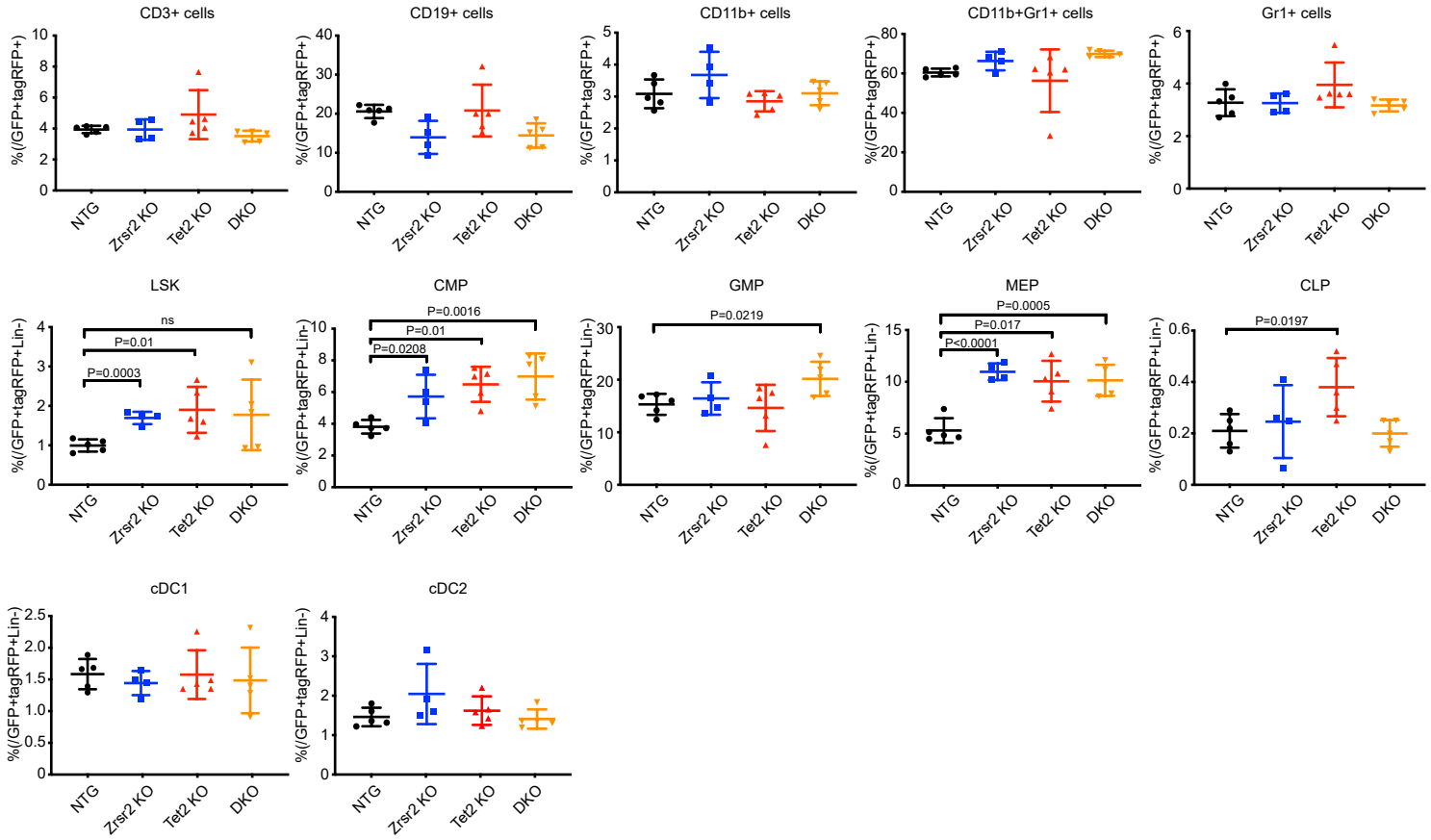

c

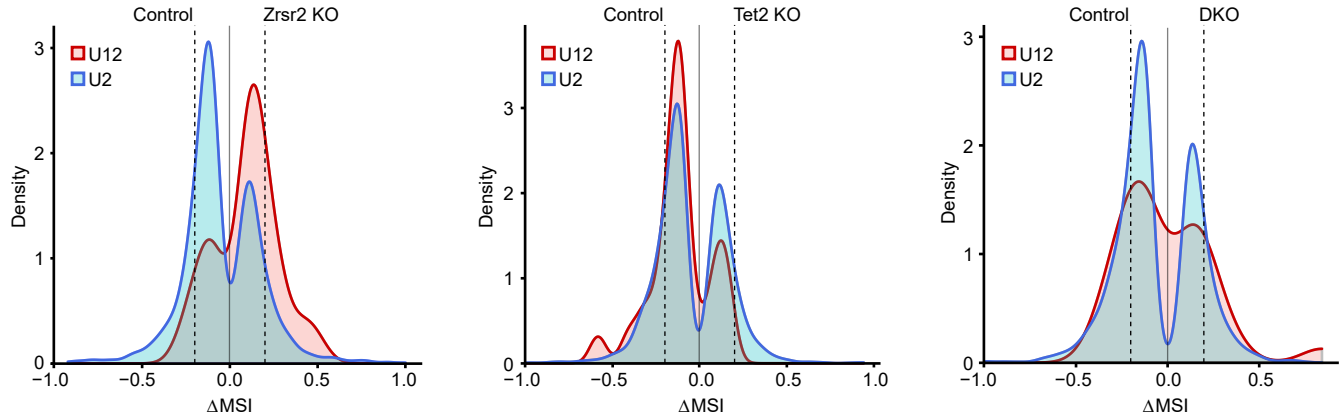

Supplementary Figure 8. In vivo consequences of *Zrsr2* and *Tet2* CRISPR/Cas9 targeting on hematopoiesis and pDC intron retention.

a. Total number of nucleated cells per two legs (femurs and tibias) in the bone marrow of recipient mice of the indicated CRISPR/Cas9 edited transplants. **b.** Bone marrow hematopoietic populations as percentage of GFP/tagRFP double positive cells in the bone marrow (top row) or of Lineage-negative GFP/tagRFP double positive cells (bottom row). Groups compared by t test. LSK, lineage-Sca1+cKit+; CMP, common myeloid progenitor; GMP, granulocyte-monocyte progenitor; MEP, megakaryocyte-erythroid progenitor; CLP, common lymphoid progenitor. **c.** Density plots of frequencies of U2-type (blue) and U12-type (red) introns among aberrantly retained introns (Fisher's exact test P-value ≤ 0.05) in pairwise analyses of GFP+/tagRFP+ pDCs from the indicated genotypes versus non-targeting control sgRNA-containing pDCs.